Interaction of unprotonated and protonated polyethylenimine with phospholipid bilayer: A molecular dynamics study

A thesis submitted towards partial fulfilment of

5 year BS-MS Dual Degree Program

by

Abhinaw Kumar

Under the guidance of

Dr. Sudip Roy

Scientist

National Chemical Laboratory, Pune

Department of Chemistry

Indian Institute of Science Education and Research, Pune

Certificate

This is to certify that this dissertation entitled “Interaction of unprotonated and protonated polyethylenimine with phospholipid bilayer : A molecular dynamics study” towards partial fulfilment of 5 year dual BS-MS program at the Indian Institute of Science Education and Research, Pune, represents original research carried out by Abhinaw Kumar under the supervision of Dr. Sudip Roy during the academic year “2011-2012”.

Abhinaw Kumar

(20071050)

Supervisor

Date:
Place:

Head (chemical Sciences)

Date:
Place:

Declaration

I hereby declare that the matter embodied in the report entitled "Interaction of unprotonated and protonated polyethylenimine with phospholipid bilayer: A molecular dynamics study" is the results of the investigations carried out by me at the Department of Physical Chemistry, at National Chemical Laboratory, Pune, under the supervision of Dr. Sudip Roy and the same has not been submitted elsewhere for any other degree.

Abhinaw Kumar

Date

Place

Acknowledgements

Foremost, I would like to express my sincere and deepest gratitude to my advisor Dr. Sudip Roy for his constant support, guidance and encouragement during the project.

I would also like to thank my fellow lab mate Chandan Kr. Choudhary for his valuable discussions and help throughout the project. I thank all the lab mates for making my stay in the lab enjoyable.

I also acknowledge my classmates Piyush, Shadab, Rahul, Danveer , Ashutosh for making this period joyful.

Last but not the least; I would like to thank my family for their unconditional support and inspiring me to achieve new level of success.

Abstract

The Interaction of Polyethylenimine with lipid bilayer has several applications in biophysical research such as transfer of DNA to the target cell. The physical process of interaction at atomistic level has not been fully understood. Here, we have studied the interaction of completely protonated PEI (at very low pH) and unprotonated PEI (at very high pH) with 1,2 dioleyl -*sn*-glycero-3-phosphocholine (DOPC) bilayer using molecular dynamics method. Both protonated and unprotonated PEI associates with the hydrophilic head group of the lipid molecule. Pore formation is observed in the bilayer when protonated PEI is inserted in to the bilayer. A single chain of unprotonated PEI doesn't significantly change the density profile and area per lipid of the bilayer. Coiled PEI makes hydrogen bonds with itself when in coiled conformation and number of hydrogen bonds with water of the lipid bilayer is lesser compared to the situation in which PEI has relatively open conformation. Protonated PEI also when associated with the one leaflet of bilayer doesn't cause to change density profile and area per lipid significantly. But when protonated PEI is inserted in the bilayer, area per lipid increase and decrease in bilayer thickness is observed.

Table of Contents

List of Figures:

Chapter 1

Introduction:

Cell membrane is an essential part of the entire living organism and is fundamental to life. It acts as a filter to regulate the entry of the molecules inside the cell and maintains an environmental difference between inside and outside of the cell. Phospholipid bilayers are the major constituents of the cell membrane.[1] It is important to understand its interaction of different molecules with bilayer due to its various applications such as drug and gene delivery. Polyethylenimine (PEI) is well known for its application as gene delivery agent into the cell.[2] In this chapter, we will discuss about structure of PEI and bilayer and importance of study of interaction between them.

1.1. Polyethylenimine:

Polyethylenimine (PEI) has polymeric structure having – (CH_2-CH_2-NH) - as repeating unit. It is a commonly used polymer in paper industry and waste water treatment. It has also found an application as gene delivery vector.[2] PEI is present in both linear and branched forms. Acid catalyzed polymerization of aziridine results in branched PEI, whereas ring opening polymerization of 2-ethyl2-oxazoline leads to N-substituted polymer, which upon hydrolysis transforms into linear PEI.[3,4] PEI has high cationic charge density potential because of availability of protonable nitrogen atom in the polymer chain. One third of the atoms of PEI are nitrogen atoms, which are capable of protonation. In biological environment, cationic charges are generated by protonation of amine group. There is a correlation between cationic charge generated and pH of the environment. For example, protonation levels of PEI are 20% and 45% at pH 7 and 5 respectively.[5] Presence of high cationic charge density allows it to interact strongly with the negatively charged molecules or groups. Due to proton sponge character of PEI, Structure of PEI is different at different pH.[6] At lower pH, PEI is highly protonated and has expanded structure while at higher pH; it is less protonated and has coiled structure.[7] pH responsive polymers, like PEI, have been used in gene delivery, because there is considerable change in pH within cellular compartments, for example a lower pH is observed in tumours (pH 6.5-7.2), lysosome (pH 4.5-5.0) and endosome (pH 5.0-6.5) in comparison to normal tissues.[5]

1.2. DOPC Lipid Bilayer:

Lipid bilayer is made up of thin bimolecular sheet of mainly phospholipid molecules. Two layers of lipid are packed such that their hydrophobic tail point inwards and their hydrophilic head are exposed to water outside. Lipid molecules have a hydrophilic head group and two hydrophobic tail groups. Hydrophilic head of a phospholipid molecule consists of choline group and phosphate group whereas hydrophobic tail is made up of long carbon chain. In our case, we have taken Dioleylphophatidylcholine (DOPC) bilayer as the model system.

a) DOPC structure: Structure of DOPC lipid is shown below. It has a hydrophilic head group (choline and phosphate group) and hydrophobic tail group (long fatty acid chain) present in it.

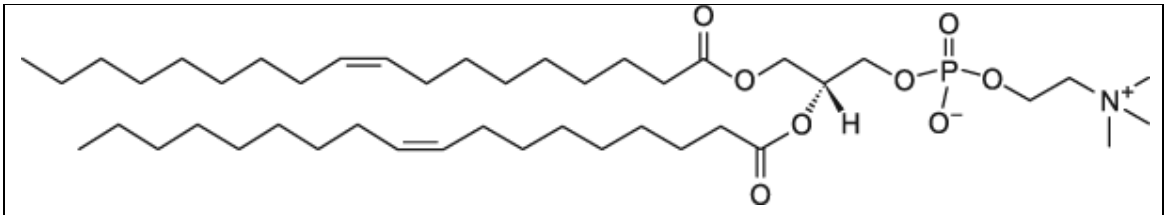

Figure 1. structure of DOPC lipid

There are two main reasons to choose DOPC bilayer as model system. DOPC structure has double bond present in its tail part. Most biological membrane contains a mixture of lipid and these lipids are generally unsaturated.[8] Transition temperature from gel to liquid phase for bilayer is higher than normal physiological temperatures for lipids with saturated tail part, such as 41.5^0C for DPPC bilayer.[9] Due to presence of unsaturated chain in lipid, melting transition temperature decreases, the bilayer maintain its size, fluidity and compressibility at normal physiological temperature.[8] Unsaturated lipid bilayer is critical for proper function of certain neural membrane.[10]

1.3. Gene Delivery:

Gene therapy is a method to treat human disease by transfer of genetic material into specific cell of a patient.[14] It is an emerging method to treat various genetic disorders such as Severe combined immunodeficiency[11], and also in treating cancer[12]. Safe

and targeted transfer of DNA into the cell is a challenge in gene therapy[13]. Viral vectors have been widely used as DNA delivery agent because of their ability to transfer their genetic material into the cell efficiently[14], but due to several limitations, like immune response against the virus, difficulty in large scale production, limitation in the size of inserting DNA, has motivated to look for non-viral vectors. Lipid based vectors, dendrimer based vectors, polypeptide vectors and nano particles are some of the widely used non-viral vectors for gene delivery.[15,16] Among a range of polycations, Polyethylenimine (PEI) has been proved to be one of the most efficient transfectent agents.[2] Negatively charged DNA forms polymer/DNA complex (polyplex) with PEI, due to strong electrostatic interaction.[17] DNA can't enter the cell without complexation with PEI, as it protects DNA from cleavage by nucleases. The polyplex enter the cell via endocytosis.[18] Due to proton sponge character of PEI[19], PEI becomes more protonated at endosomal pH, that triggers the influx of water inside the endosome, resulting in swelling and rupture of endosome and polyplex gets free into the cytosol.[20,21] However the exact mechanism of polyplex movement is not fully understood, But, it is known that DNA is delivered in to the cell and PEI is free in the cytosol.[22] Now, Free PEI can interact with bilayer to induce interesting changes in the membrane bilayer properties.

1.4. Previous Study:

It has been shown that polymer interacts with membrane bilayer via hydrophobic and hydrophilic interaction, coulombic association or hydrogen bond, depending on the structure of the polymer.[23] Polycations interact with membrane bilayer via electrostatic interaction and deform the bilayer or binds strongly with the hydrophilic part of the bilayer. Interaction of zwitterionic lipid vesicles with PEI molecule was studied by Sikor et al.[24] It was shown that at low salt concentration, aggregation of zwitterionic lipid vesicles takes place with formation of stable clusters while at high salt concentration, no aggregation of vesicles happen and PEI is able to penetrate into the membrane bilayer. To better understand these experimental studies at atomistic scale, we need to perform molecular dynamics simulation. Coarse grained molecular dynamics simulation study by Lee and Larson for the interaction of interaction PAMPAM dendrimer with lipid bilayer shows that charged dendrimer deform and insert into the bilayer but uncharged dendrimer is not able to penetrate

into the bilayer.[25] A study of interaction of modified cation poly(allyl-N, N-dimethyl-N-hexylammonium chloride) with POPC bilayer was done and pore formation was observed in the membrane bilayer that enabled movement of water molecules and ions across the membranes.[26]

1.5. Motivation of the present Study:

In this study, we have performed atomistic molecular dynamics simulation study of interaction of unprotonated and completely protonated PEI with 1, 2-dioleyl-sn-glycero-3-phosphocholine (DOPC) lipid bilayer. As PEI has both hydrophobic (C-C part) and hydrophilic (N) atoms present in it, it would be interesting to find the attachment site of PEI with the lipid bilayer which has hydrophilic head and hydrophobic tail group. Polycations have been used as drug delivery agent due to their activity as antimicrobial agent. We shall also investigate whether protonated PEI can form the pore into the bilayer. We have taken two different conformation of PEI, linear and coiled, to take into account the effect of pH on PEI in coiled form is representative of high pH (basic environment) and PEI with complete protonation is in linear form which is representative of low pH (acidic environment). Interaction of PEI structure at different pH with bilayer will give insight into attachment of polymer with the bilayer. Interaction of protonated PEI will give an insight in to endosome rupture activity during gene delivery, which has implications in designing better transfectent agent, and also it will lead to a better understanding of interaction of free PEI with membrane bilayer after the gene delivery. It has been hypothesized that endosome rupture activity is observed due to proton sponge character of PEI. At lower pH inside the endosome, PEI attracts water inside the endosome and there is disruption of endosomal structure.[20,21] It will be investigated whether a PEI chain is able to attract water in the inner region of the phospholipid bilayer. We will try to find the favourable site of attachment of PEI with the phospholipid bilayer and find out whether PEI can induce pore formation in the bilayer. The change in bilayer structure due to presense of PEI will also be studied. Till date, no molecular dynamics study has been done to study the interaction of pH dependent structure of PEI with membrane bilayer.

Chapter 2

Initial Structures:

Five systems were prepared by incorporation of PEI in different regions of the lipid bilayer. Simulated annealing was performed to obtain the structure of 20-mer PEI (both completely protonated and unprotonated) at 310K for insertion at different positions in the bilayer. Equilibrated DOPC bilayer containing 72 lipids was obtained from previously reported work of Siu et al.[27] Structure was replicated to obtain lipid bilayer with 144 DOPC molecule. Water was removed from above and below the equilibrated structure of the bilayer. Two structures were made with unprotonated PEI and protonated PEI positioned above the bilayer away from the head group region of the lipid molecule. Now, both coiled and linear PEI was translated along the normal of the bilayer to place it in the middle part of the bilayer in the hydrophobic region. And in the fifth structure linear protonated PEI is placed is placed along the normal of the bilayer. Each of the structure is energy minimized using steepest descent technique. Then, a layer of water is added to both side of the bilayer, so that lipid molecules are well solvated. Thus, we have five systems, in which first two structures are prepared by adding coiled PEI with the lipid bilayer. PEI placed above the bilayer in the water is named system A and system with coiled PEI present in the inner hydrophobic region of the bilayer was named system B. Whereas system with protonated PEI placed above the head group, in the hydrophobic region of the bilayer, and along the normal of the bilayer, are named system C, D and E respectively. Numbers of water molecules added in system A, B, C, D and E were 6995, 7065, 6969, 7048 and 8748 respectively. Extra water was added to system E to keep lipid head group well solvated after long time of simulation, as water flows through the bilayer after some time in this system. Chloride ions were added in systems C, D and E to neutralize the charge present in the systems.

System A and B

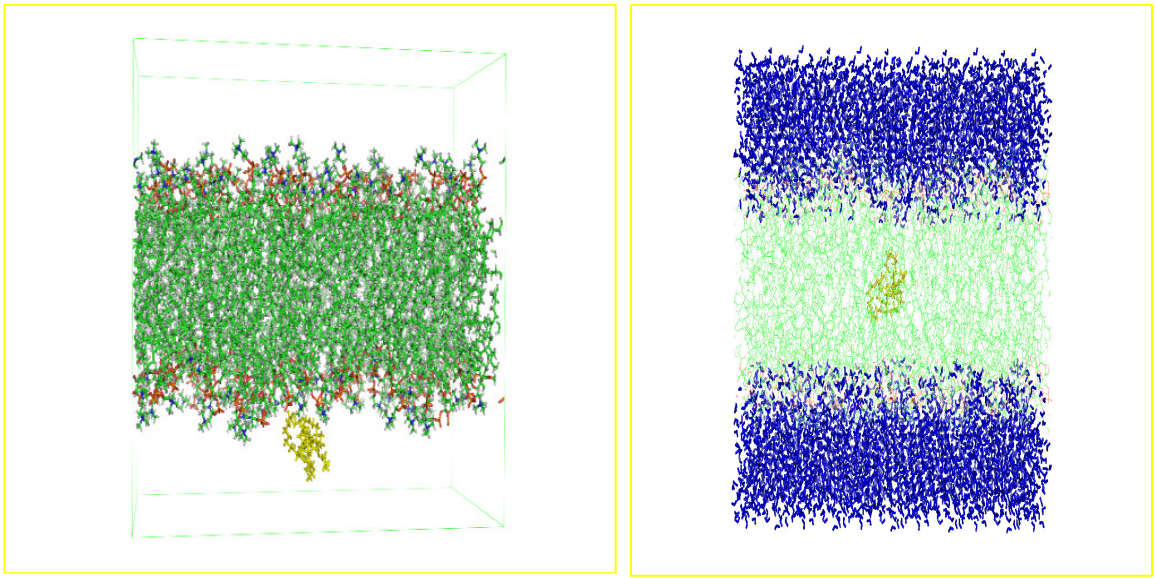

Figure 2. Initial structure of system A and B

As shown in figure 2, system A and B were prepared by placing PEI in water near to the hydrophilic head of the bilayer. Unprotonated PEI was placed in water and slightly away from the hydrophilic head of the bilayer. Initial positions were biased towards hydrophobic head group in system A and towards hydrophobic tail group in system B. As we were doing simulation for only 150ns, biased initial position will allow unprotonated PEI to cover almost all possible position in the lipid bilayer region. These two systems were prepared to find the favourable site of attachment of unprotonated PEI with the lipid bilayer.

System C, D and E: [Figure 3]

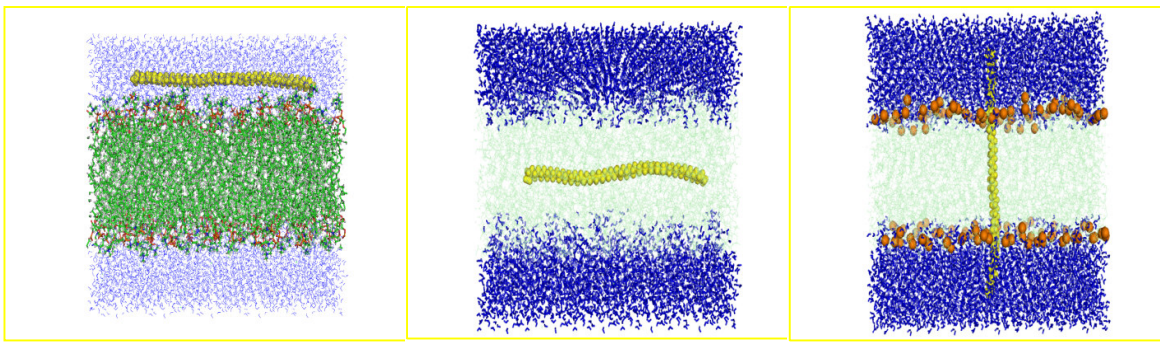

As shown in figure 3, protonated PEI is placed at three different initial positions in system C, D and E. PEI was present in water near the hydrophilic head groups of the bilayer, and it was present in the hydrophobic region of the bilayer in the system D. Where as in system E, protonated PEI was placed such that part of the protonated PEI is facing water and some part of the PEI is in the hydrophobic region of the bilayer. Different initial structures were made to allow PEI to cover almost all possible positions in the bilayer region. System D was made to see whether PEI can pull water inside and remain stable in the hydrophobic region of the bilayer. System E was prepared to find out whether a stable pore can be formed around PEI in the bilayer.

Molecular dynamics simulation was performed on all the five systems mentioned above. Here, Methods employed for molecular dynamics simulation have been described.

2.2. Molecular dynamics Method:

Molecular dynamics is a principal tool in treating the biological system and also in material science. Here, all the systems are simulated using classical mechanics laws. Interactions between atoms are divided in to bonded and non-bonded interaction. Non bonded interaction is between pair of atoms not connected by chemical bond and is within a cutoff radius. Bonded interaction is defined between atoms, which are connected by chemical bond. Nonbonded interactions are mainly of two types: van der wall interaction and electrostatic interaction. Charge and nonbonded parameter for attraction and repulsions are assigned for each atom in the system. The bonded interaction has mainly three parts: Bonded, angle and dihedral terms.

The general formula for potential includes terms for bonded and nonbonded potential is given by equation 1.

$$V = \sum_{i<j} \frac{q_i\, q_j}{4\pi\varepsilon_o r_{ij}} + \sum_{i<j} \frac{A_{ij}}{(r_{ij})^6} - \frac{B_{ij}}{(r_{ij})^6} + \sum_{bonds} \frac{1}{2} K_{ij}^{b} (r_{ij} - b_{ij}^{o})^2 + \sum_{angles} \frac{1}{2} K_{ijk}^{\theta} (\theta_{ijk} - \theta_{ijk}^{o})^2 + \sum_{dihedrals} K_{\varphi}\left(1 + \cos\left(n(\varphi - \varphi^{o})\right)\right) \quad (1)$$

Where r_{ij} is the distance between pair of atoms i and j, q_i and q_j are the partial charges on atom i and j, A_{ij} and B_{ij} are the Leonardo Jones parameters, K_b, K_θ and K_φ are the force constant for bond, angle and dihedrals. $b_{ij}^o, \theta_{ijk}^o, \varphi^o$ are equilibrium bond length, bond angle and dihedral angle respectively.

First two terms are for non-bonded interaction and last three terms are bonded interactions.

2.2.1 Force-field: The force field provides the description of interaction as in equation 1.Simulation packages force-field provides the specific form of above equations and various parameters involved. There are various force field types available such as AMBER[28], CHARMM[29] GROMOS[30], and OPLS-AA[31]. We have used General AMBER force field for simulating our systems.

2.2.2 Global MD algorithm[32]:

1. Input Initial conditions

Potential interaction V as a function of atom position

Positions r and velocities v of all atoms of the system

↓

Repeat step 2, 3, 4 for require dumber of steps:

2. Compute Forces

The force on any atom

$$F_i = -\frac{\partial V}{\partial r_i} \qquad (2)$$

Is computed by calculating the force between non bonded atom pairs:

$$F_i = \sum_j F_{ij} \qquad (3)$$

plus the forces due to bonded interactions, plus restraining and external forces.

↓

3. Update Configuration

The movement of the atoms is simulated by numerically solving Newton's equation of motion

$$\frac{d^2 r_i}{dt^2} = \frac{F_i}{m_i} \qquad (4)$$

↓

4. Output step

Write positions, velocities, energies, temperature, pressure, etc.

2.2.3 Periodic boundary Condition[32]:

Periodic boundary condition (PBC) is applied to minimize the edge effect in a finite system. The PBC is imposed by putting all the molecules to be simulated in a box and then translate the copy of the box along a particular direction for PBC along that direction. In GROMACS, PBC is used along with the minimum image convention ie. Only the nearest image of each particle is considered for short range non bonded interaction terms. While for long range interaction, it incorporated lattice sum methods such as Ewald Sum, PME, and PPPM.

2.2.4. Cut-off restriction:

As the minimum image convention has been applied, a cut-off radius is used to truncate non-bonded interactions so that not more than one image is within the cut-off distance of the force.

2.2.5. Leap frog algorithm[33]:

Leap-frog algorithm is default method for integration of equation of motion in GROMACS. The leap-frog algorithm uses position r at time t and velocities v at time $t - \frac{1}{2}\Delta t$; positions and velocities are updated using the force F(t) determined by position at time t:

$$r(t + \Delta t) = r(t) + \Delta t\, v(t + \frac{1}{2}\Delta t) \qquad (5)$$

$$v(t + \frac{1}{2}\Delta t) = v(t - \frac{1}{2}\Delta t) + \frac{\Delta t}{m} F(t) \qquad (6)$$

The stored quantity are the current position r(t), acceleration a(t) and the velocities v(t $-\frac{1}{2}\Delta t$) at mid steps. The velocity equation is implemented first, and the velocities leap over the coordinates to give next mid-step values v(t $+\frac{1}{2}\Delta t$). Current velocity during the time can be calculated as

$$v(t) = \frac{1}{2}\,(v(t + \frac{1}{2}\Delta t\,) + v(t - \frac{1}{2}\Delta t)) \qquad (7)$$

It is essential so that energy (kinetic + potential) as well as any other quantity which require position and velocity at same time can be calculated at time t. The algorithm is time reversible.

2.2.6. Constraints:

LINCS[34] or SHAKE[35] algorithm is used in GROMACS for constraints. In our simulation, we have used LINCS algorithm which reset bonds to their correct length after an unconstrained update. The description of the algorithm is beyond the scope of this thesis.

2.2.7. Simulated Annealing[36]:

Annealing is a process in which a single large crystal is obtained upon slowly reducing the temperature of a molten material. The crystal obtained corresponds to global minimum of free energy. Simulated annealing is a computational method inspired from the process, finds the best solutions for a problem having large number of possible solution (Kirkpatrick et.al. 1983). Simulated annealing is used in conformational analysis of a molecule where internal energy is the cost function and temperature is the control parameter. System is allowed to reach to a minimum of energy at a particular temperature using molecular dynamics or monte-carlo method. At higher temperature, system is able to cross over high energy barriers and high energy conformation becomes available. While at lower temperature, lower energy states are more probable according to Maxwell-Boltzmann distribution. Infinite number of steps will be required to find a global minimum and system should come to equilibrium at each of those steps. In our case, we have performed simulated annealing for the PEI and have extracted the PEI structure from near the end of the

20ns simulation corresponding to the temperature of 310K. It was done to find the unbiased conformation of PEI at 310K.

2.2.8. Energy minimization[32]:

Energy minimization in GROMACS can be done using steepest descent[32], conjugate gradient[32] or l-bgf[37] method. In our simulation we have used steepest descent method for simulation.

Here, we define a vector r as the vector of all 3N coordinates. Now, a maximum displacement h_0 is given and force F as well as potential energy is calculated. New position is given by:

$$r_{n+1} = r_n + \frac{F_n}{\max(|F_n|)} h_n \qquad (8)$$

Where F_n and h_n are the force and the maximum displacement respectively.

$\max(|F_n|)$ denotes the maximum of the absolute value of the force components. Now, forces and energy are again computed for new positions.

If ($V_{n+1} < V_n$) the new positions are accepted and $h_{n+1} = 1.2\ h_n$.

If ($V_{n+1} \geq V_n$) the new positions are not accepted and $h_n = 0.2h_n$

The algorithm stops when the maximum of absolute value of force component is smaller than a specified value ϵ or when it reaches the number of specified steps by the user. Value of ϵ between 1 and 10 is acceptable.

2.2.9. Position restraints[32]:

It is used to restrain particles to fixed reference positions R_i. These are used during equilibration to avoid sudden changes in critical part such as restrain motion of protein from large solvent forces when the solvent is not yet equilibrated. The following form has been used:

$$V_{pr}(r_i) = \frac{1}{2} K_{pr} |r_i - R_i|^2 \qquad (9)$$

Potential can be written in the form of:

$$V=\frac{1}{2}[K_{pr}^{x}(x_i-X_i)^2+K_{pr}^{y}(y_i-Y_i)^2+K_{pr}^{z}(z_i-Z_i)^2\ ] \qquad (10)$$

Now the forces are:

$$F_x^i = -K_{pr}^{x}(x_i-X_i) \qquad (11)$$

$$F_y^i = -K_{pr}^{y}(y_i-Y_i) \qquad (12)$$

$$F_z^i = -K_{pr}^{z}(z_i-Z_i) \qquad (13)$$

Using different force constants in each direction, we can restrain the position in the desired direction. Position restraint is applied to a fixed set of atoms.

K_{pr}^{x}, K_{pr}^{y} and K_{pr}^{z} were equal to 1000 N/m during position restraint in our simulation.

Position restraint was applied for all the system for initial few nanosecond of simulation. It was done to ensure that molecules surrounding PEI molecule adjust themselves such that there was no sudden change in position of PEI when solvent were not yet equilibrated.

2.2.10. Temperature Coupling:

There are several methods to keep constant temperature in constant temperature ensemble (ex. NPT, NVT) such as Brendensen temperature coupling[38] Velocity rescale coupling[39] and Nosé-hoover scheme.[40,41] In our simulation we have used Brendensen temperature coupling.

Brendensen temperature coupling algorithm does weak coupling with an external bath at temperature T_0 according to first order kinetics. The deviation of system temperature from T_0 is corrected using the formula:

$$\frac{dT}{dt}=\frac{T_0-T}{\tau} \qquad (14)$$

The equation implies that deviation in temperature will show exponential decrease with time constant τ. This coupling method has advantages such as strength of coupling can be changed depending upon our use. We can take shorter coupling

time for initial equilibration (like 0.01 ps) but for production run we can use larger coupling time (such as 0.5 ps).

2.2.11. Pressure Coupling[33]:

A system can be coupled to pressure bath in the same way as temperature bath. Brendensen algorithm and MTTK algorithm are implemented generally for pressure coupling. We have used surface tension coupling which uses Brendensen algorithm.

In Brendensen algorithm, coordinates and box vector are rescaled with a matrix μ on every step which results in first order kinetic relaxation of pressure to a reference pressure P_o:

$$\frac{dP}{dt} = \frac{P_o - P}{\tau_p} \qquad (15)$$

The scaling matrix μ is represented by:

$$\mu_{ij} = \delta_{ij} - \frac{n_{pc}\,\Delta t}{3\tau_p}\beta_{ij}[P_{0ij} - P_{ij}(t)] \qquad (16)$$

β is defined as isothermal compressibility of the system.

In simulation of periodic system having more than one phase and separated by surface parallel to the xy plane, surface tension and the z-component of the pressure can be coupled to a pressure bath. Pressure is corrected using Brendensen algorithm described above.

The average surface tension is calculated from difference between normal and lateral pressure:

$$\gamma(t) = \frac{1}{n}\int_0^{L_z}\{P_{zz}(z,t) - \frac{P_{xx}(z,t)+P_{yy}(z,t)}{2}\}dz \qquad (17)$$

$$= \frac{L_z}{n}\{P_{zz}(z,t) - \frac{P_{xx}(z,t)+P_{yy}(z,t)}{2}\} \qquad (18)$$

Here, L_z and n are the height of the box and the number of the surfaces respectively.

The correction of pressure in z-direction is done by scaling the height of the box in z-direction by μ_z:

$$\Delta P_{zz} = \frac{\Delta t}{\tau_p}\{P_{0zz} - P_{zz}(t)\} \quad (19)$$

$$\mu_{zz} = 1 + \beta_{zz}\,\Delta P_{zz} \quad (20)$$

Now, using the pressure correction in z-direction, surface tension value is subjected to converge to the reference value γ_0.

The correction factor for box length in x/y-direction is given by:

$$\mu_{x/y} = 1 + \frac{\Delta t}{2\tau_p}\beta_{x/y}\left(\frac{n\gamma_0}{\mu_{zz}\,L_z} - \{P_{zz}(z,t) + \Delta P_{zz} - \frac{P_{xx}(z,t)+P_{yy}(z,t)}{2}\}\right) \quad (21)$$

2.3. Computational Details:

The MD simulations were performed using the GROMACS 4.5.4 package[42]. The periodic boundary conditions were applied in all directions. The systems were coupled to a temperature bath at 310K with a coupling time constant of 0.1ps^{-1} [43]. Systems were simulated at constant pressure applying a pressure coupling with relaxation time of 1ps at a pressure of 1bar. Surface tension of 22dyne/cm/surface was applied to ensure that area per lipid is in agreement with the experimental value. All systems were simulated under NPγT ensemble. Bonds to H atoms were constrained using the LINCS[44] algorithm for lipids and H-bonds for water were constrained using SETTLE[45] algorithms allowing for an integration time step of 2 fs. The non bonded pair list was updated every 10 steps with a cut off of 1.0 nm. For the short range van der wall interactions, a cut off distance of 1.0 nm was used. The long range electrostatics potential was calculated using Particle Mesh Ewald (PME) method with a grid spacing of 0.12 nm and cubic interpolation was adopted. Volume compressibility was chosen to be 4.5 x 10^{-5}bar^{-1}. All atomistic GAFF[28] (General Amber Force Field) was used. Charges on atoms of DOPC and PEI molecule were taken from previously reported work by Siu et al.[27] and Kumaraswamy et al.[7] respectively. TIP3P model of water has been used in the simulation.[31] The data were collected every 1ps of the simulation. Initially, PEI was position restrained for 4ns in system A, B and C and for 500ps for system D and E, so that it PEI is well solvated

by water molecule. Water is position restrained to move only in xy plane perpendicular to normal of the bilayer in case of system D and E to stop water from entering inside the bilayer from the very beginning of the simulation. The time step and relaxation time for the simulation during position restraint of PEI for system A, B and C was 1fs with relaxation time 1 s^{-1} while for system D and E, those numbers were 0.5fs and 10s^{-1} respectively. Now, position restraints were removed and all the simulations were extended for 150ns.

Chapter 3

Results:

3.1. Partial density:

All the analysis was done for the last 50 ns from the 150 ns simulation.

Partial density is mass per unit volume for a particular set of molecules. Partial densities for DOPC, Water and PEI for each system were calculated along the z-direction towards the normal of the bilayer. The graphs were shifted by appropriate distance such that one end of interface is same for all the systems.

3.1.1. Unprotonated PEI with bilayer:

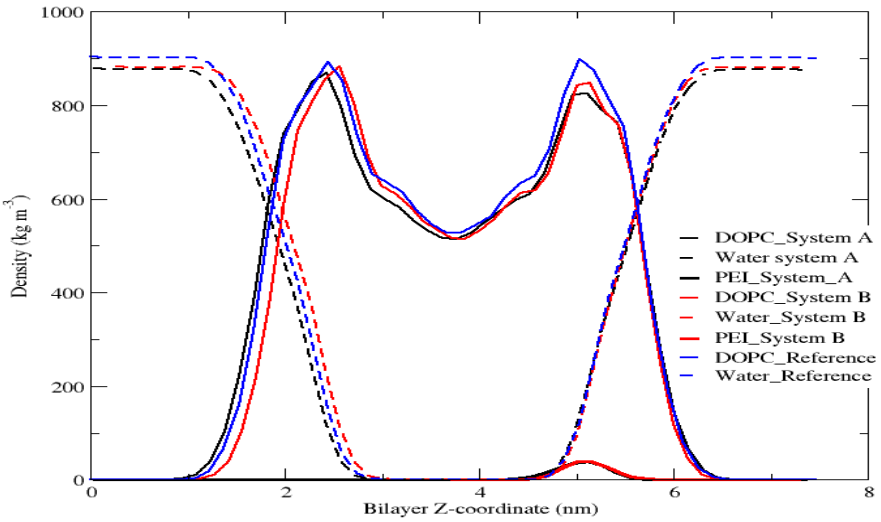

Figure 4. Partial density plot for system A, B and reference system (without PEI)

Partial density plot shows that there are three regions in the bilayer. The first region is broad where only water molecules are present. Second region is interfacial region where both water molecule and lipid head group is present. Density of water molecule starts to decrease in this region and in third region has no water molecules and only tail group of DOPC molecule are present.

It is observed that unprotonated PEI is present at the same position in the interfacial region of the bilayer in case of both system A and B, after 150ns of the simulation. Though, we had started with the different position of coiled PEI in the system A and B. For system A, PEI was positioned in the water above the lipid group. After the few nanosecond of simulation, a part of PEI started interacting with the head group region (figure 23 & 24) and slowly, complete PEI structure got attached to lipid head group (figure 23 & 24) and it stays there till the end of the simulation. It was true for the both the system A and B. It means that interaction of PEI with lipid head is more favourable than the interaction of PEI with water and the hydrophobic tail. There is no significant change in the density profile of water and DOPC molecule upon interaction of the single chain of PEI with the bilayer. That means that a single chain of unprotonated PEI is not able to bring any drastic change in the bilayer structure.

3.1.2. Protonated PEI with bilayer:

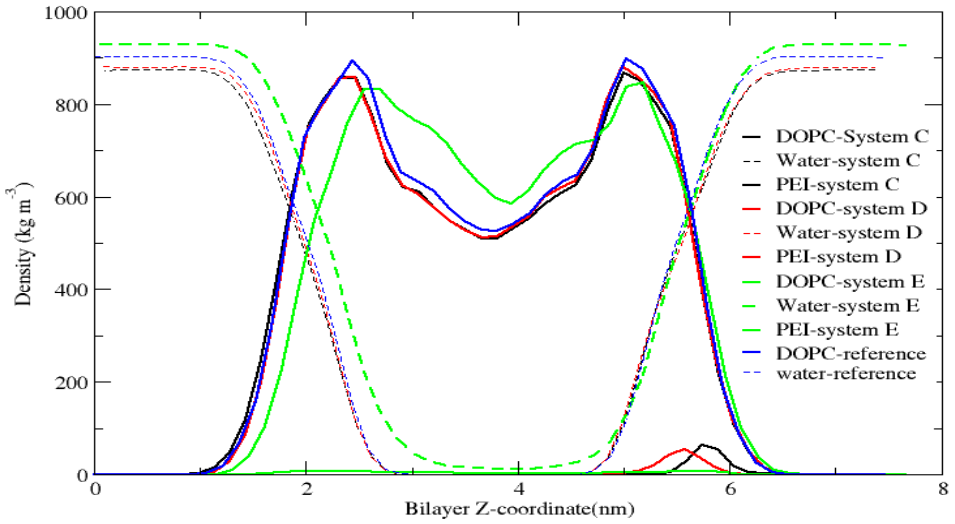

Figure 5. Partial density plot for system C, D and E.

It was observed that the partial density profile for DOPC and water in case of system C and D were same as reference system without any PEI. A decrease in width of

bilayer was observed for the system E compared to reference system. There is finite density of water molecules in the hydrophobic region of the bilayer for system E. However density of water molecule is zero in the apolar core region of the bilayer for any other system. There is also a decrease in the peak value for DOPC at the interfacial region and the peak value in the middle of bilayer increases indicating that there is a change in orientation of the lipid molecules in case of system E. The peaks for partial density of protonated PEI are slightly different. Protonated PEI The protonated PEI in system D is present deep inside the interfacial region of the bilayer whereas protonated PEI in system C has not gone deep into the interfacial region of the bilayer.

We started the simulation by placing Linear PEI in water and slightly away from the lipid head group in system C (figure 25), and by positioning in the hydrophobic region in the system D (figure 26). But in the equilibrated configuration linear PEI is present in the hydrophilic region of the bilayer in both the system C and D. In system D, as soon as simulation is started, the PEI molecule has tendency to move in the direction towards the lipid head group. Water molecule flows through the membrane to solvate the protonated PEI very quickly (figure 26). But after around 8ns of simulation, the PEI molecule was completely shifted towards one leaflet of the bilayer, and the pore formed along the bilayer vanished. The stoppage of flow of water along the bilayer may be due to the fact that interaction of protonated PEI with hydrophilic head group is favourable than the hydrophobic interaction with the tail group of the lipid, So, protonated PEI was shifted towards lipid head group, and when it is completely into one leaflet of the bilayer, it is solvated by water molecules of that leaflet of the bilayer and the movement of water across the membrane stops. A stable pore formation is observed in case of system E where water flows through the bilayer. From the density graph for system E, protonated PEI is tilted towards the lipid head group of the bilayer and is linear in the hydrophobic region of the lipid bilayer. Significant number of water molecules is flowing through the bilayer. It can be said that energy required to overcome hydrophobicity of lipid tail group is compensated by the energy released by solvation of the protonated PEI.

3.2. Area per Lipid: The area per lipid was calculated as lateral area of the simulation box (the xy plane) divided by number of lipids in one monolayer (72 in our case).

3.2.1 Unprotonated PEI with bilayer

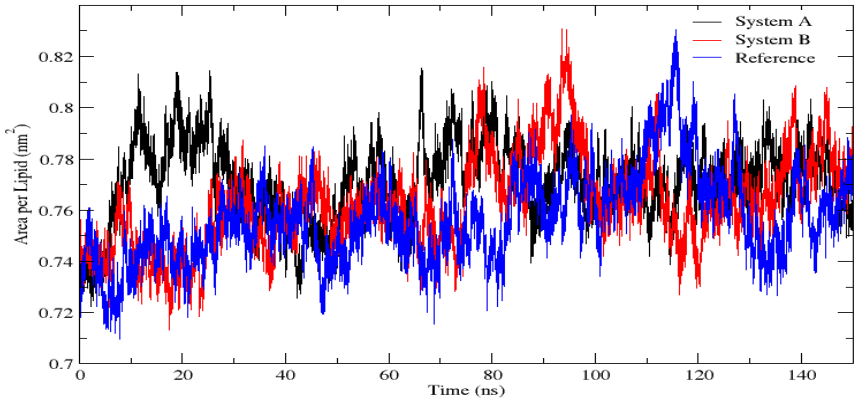

Figure 6. Area per lipid for system A and B with respect to time.

Area per lipid is found to be almost independent on the presence of PEI molecule in the bilayer. Average area per lipid is 0.77±0.02 nm^2 in system A and 0.76±0.02 nm^2 in system B. This is almost same as reference system (only bilayer system) which has area per lipid equal to 0.76±0.02 nm^2. Experimental study suggests an area per lipid of DOPC bilayer equal to 0.721 nm^2, which is in good agreement with simulated value. No change in area per lipid compared to reference due to presence of a single chain of unprotonated PEI suggest that lipid bilayer structure remains intact when a single chain of PEI molecules interacts with the lipid bilayer.

3.2.2. Protonated PEI with bilayer

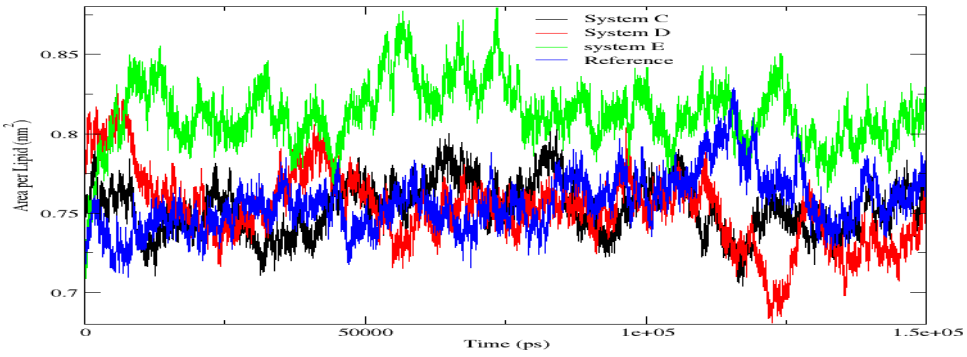

Figure 7. Area per lipid for systems C, D and E with respect to time.

Area per lipid for PEI in water and PEI in bilayer case was same equal to 0.75±0.02 nm^2 was same for all the cases except when PEI was present along the normal to the bilayer, where an increase in area per lipid was observed due to movement of water molecule along the pore formed in the bilayer. Area per lipid in this case was found to be equal to 0.81±0.02 nm^2 which is significantly higher than other cases.

Polymer properties: All the calculation has been done for last 50 ns from the complete 150 ns of simulation

3.3. Unprotonated Case:

3.3.1. End to end distance distribution:

For PEI, End to End distance has been defined as distance between 1st and 20th carbon of the 20-mer PEI chain.

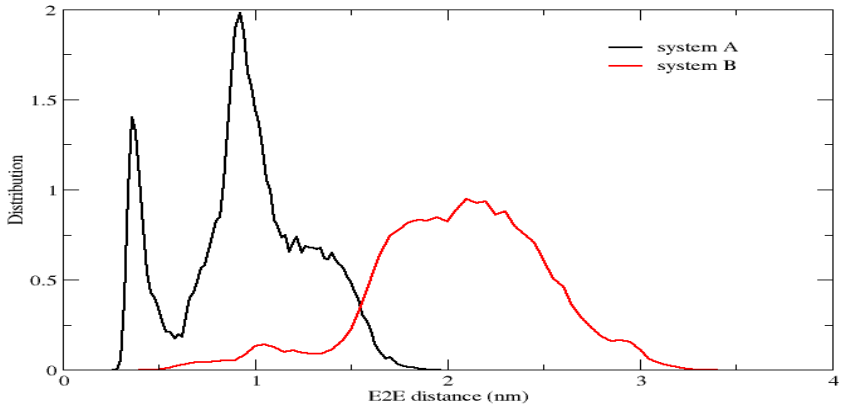

Figure 8. End to end distance distribution of unprotonated PEI in system A and B

End to end distance between 1st and 20th carbon of unprotonated PEI is in the range of 0.25 nm to 3.5 nm in both the system A and B, representing the coiled conformation of PEI. The unprotonated PEI remains in coiled conformation in the interfacial region of the bilayer.

From the end to end distance (E2E) distribution plot of PEI for system A and B, it can say that structures of PEI are different though density plot suggests that they are at the same position in the bilayer. The average E2E distance for PEI in System A and B are 0.95 $\pm$ 0.34 nm and 2.06 $\pm$ 0.44 nm respectively. The E2E distance is lower for unprotonated PEI in system A, indicating a closed conformation where as a larger E2E distance for PEI in system B signifies an open structure of PEI. There is a broad peak when unprotonated PEI is placed inside the bilayer as initial structure whereas for the other case; we have a relatively narrow distribution. By observing the snapshot from the simulation, it was seen that half part of the PEI is attached to the bilayer and other half part is flexible leading to higher E2E distance. While as in system B, PEI has closed conformation, and is attached to the hydrophilic head of the lipid molecule. It can be said that in equilibrium structure conformation of PEI in the head group region is dependent on the conformation of PEI while entering the bilayer. And it can be concluded that there are two stable conformation of PEI in the lipid head group region of the bilayer.

3.3.2. R_g distribution

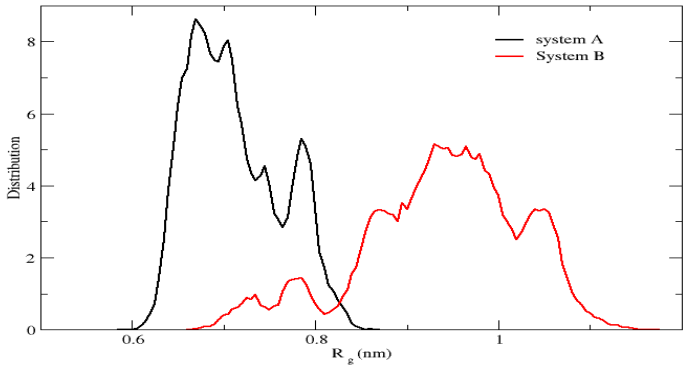

Figure 9. Radius of gyration distribution of unprotonated PEI in system A and B

R_g plot for unprotonated PEI shows that R_g of PEI is less in system A than in system B. Average of R_g for PEI in system B was found to be 0.93 $\pm$ 0.09 nm, whereas It was equal to be 0.71 $\pm$ 0.05 nm for system A. That implies that PEI has more coiled conformation in system A than in system B. It can be clearly seen by the snapshots

taken at end of the simulation as shown in figure 23 &24. It is also consistent with the E2E distribution plot, which suggest that PEI in system A has closed structure where as PEI has open structure in case of system B. R_g of unprotonated PEI in system B has a large distribution indicating a fluctuation in structure, is supported by the fact that it has an open structure and one end of the PEI has larger movement.

3.3.3. Lateral Diffusion of PEI

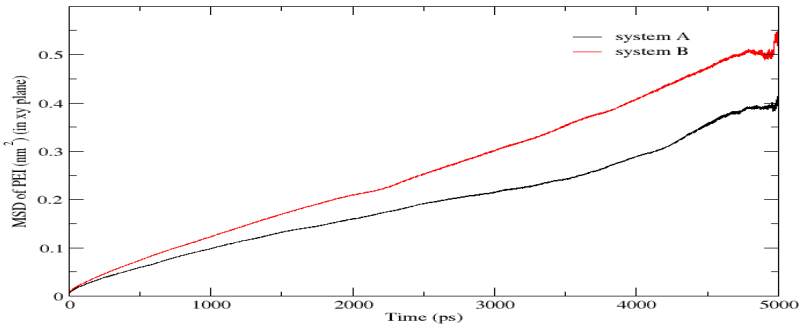

Figure 10. Mean square displacement of unprotonated PEI in xy plane in system A and B

Lateral diffusion of unprotonated PEI was calculated in the plane perpendicular to normal of the bilayer (i.e. in the xy plane perpendicular to z-axis). Lateral mean square diffusion of coiled PEI was found to be more in case of PEI in the system B where it was present in open conformation than in the closed conformation in the system A. It also supports all previous result which tells that there is more fluctuation in structure of PEI where it has open conformation. The lateral diffusion graph is not linear as there is only one chain of PEI is present and hence has less statistical data. So, we can't calculate lateral diffusion constant here. We have only compared the value of mean square displacement with time.

3.4. Protonated Case

3.4.1. End to end distance distribution

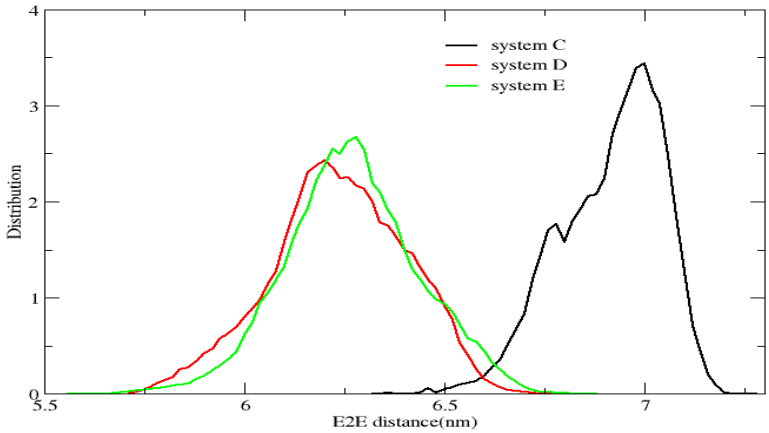

Figure 11. End to end distance distribution of protonated PEI in system C, D and E

It is observed that in system C, where PEI was present in water as initial structure, it doesn't go very deep inside the hydrophilic part of the lipid molecule compared to system D. The average E2E distance in system C, D and E were 6.83 $\pm$ 0.20 nm, 6.23 $\pm$ 0.17 nm, and 6.26 $\pm$ 0.16 nm. The E2E distance for protonated PEI is larger than in system D and E, indicating that conformation of PEI is in more elongated form when it is away from the hydrophilic region than when it is in the environment of phosphate and choline group. The average E2E distance is almost same for both system D and E.

We had started with elongated conformation of protonated PEI as initial conformation. The protonated PEI in system C doesn't go deep inside the bilayer as seen from the density plot shown in figure 25. The protonated PEI structure remains elongated when it is not going deep into the interfacial region of the bilayer. In case of system D, protonated PEI molecule is present deep into the interfacial region of the bilayer and it has a lower end to end distance compared to system C, indicating a contraction in configuration of PEI in presence of surrounding hydrophilic head group of the bilayer. In case of system E, where PEI has caused to change the orientation of lipid as shown in figure 27, the E2E distance is almost same as in system D.

3.4.2. R_g Distribution: all the calculations were done for last 50ns from the complete 150ns simulation.

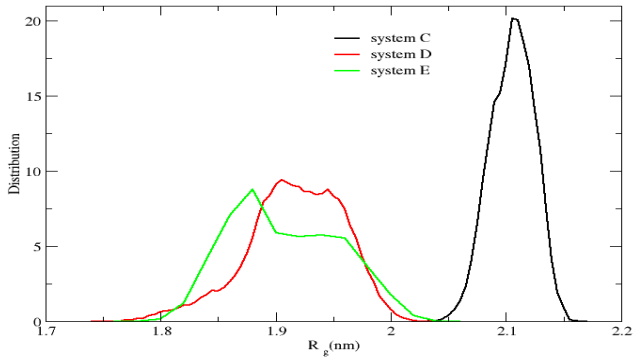

Figure 12. Radius of gyration distribution plot of protonated PEI in system C, D and E.

R_g of protonated PEI is more in system C due to elongated conformation of PEI, where as the there is decrease in R_g when it was surrounded by phosphate and choline group. The PEI present in system C was elongated more than in other two systems D and E. The average R_g of PEI in system C, D and E were 2.08± 0.03 nm, 1.91±0.04 nm and 1.91±0.03 nm respectively. The R_g distribution is almost same for system D and E. It is consistent with the trends in the E2E distribution.

If we compare the radius of gyration of protonated PEI with unprotonated PEI, the radius of gyration has higher value for protonated system implying an elongated conformation of PEI. Protonated PEI remains in elongated conformation in case of all the three system C, D and E whereas unprotonated PEI has coiled conformation in system A and B.

Radial distribution function:

Water around backbone of PEI chain

Radial distribution functions were calculated to compare the water surrounding the PEI backbone (N-C-C) in each case. Calculation has been done for the last 50ns from the 150ns simulation.

3.5.1. Unprotonated Case:

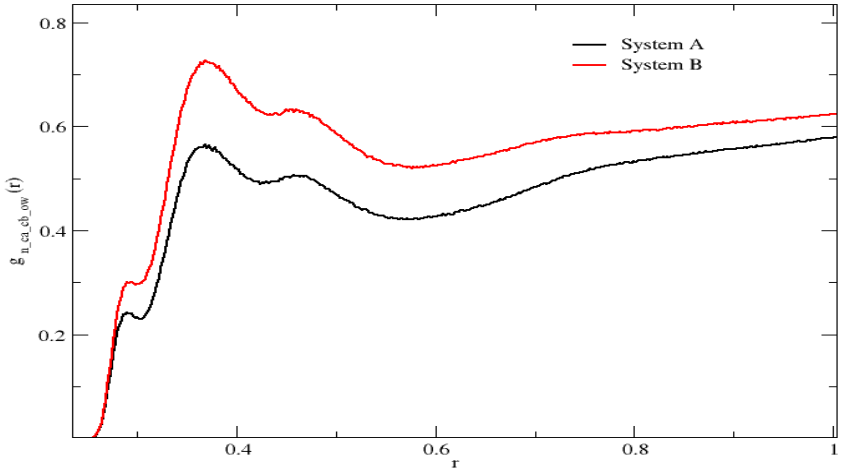

Figure 13. Radial distribution function plot for the backbone of unprotonated PEI (N-C-C) with oxygen of water molecules.

Radial distribution function of water around back bone of PEI (i.e. N-C-C) shows three peaks at 0.289 nm, 0.367 nm and 0.457 nm. The first and third peaks correspond to N-OW distance whereas second peak corresponds to C-OW distance. A higher peak value was observed for system B than for system A. That means that It is consistent with the fact that PEI in system A has more coiled conformation and surrounded by less number of water molecules. Whereas PEI in system B has open conformation and one part of PEI higher movement and hence surrounded by more number of water molecule.

3.5.2. Protonated Case: All calculation has been done for last 50ns from the 150ns simulation.

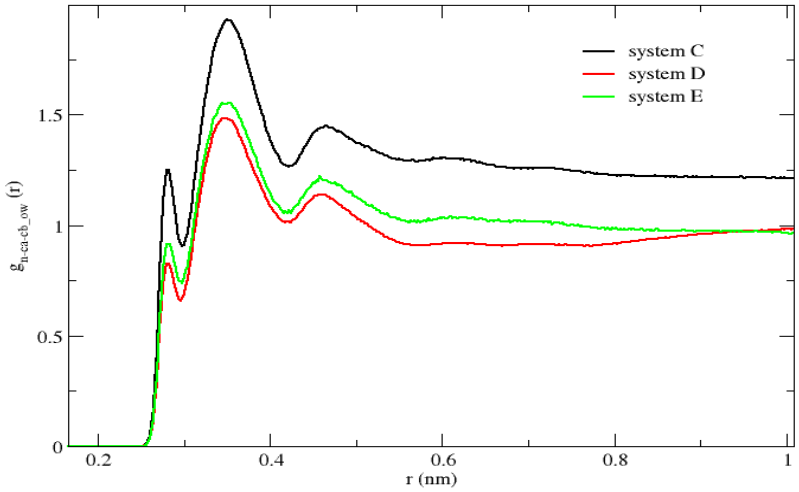

Figure 14. Radial distribution function plot for backbone of protonated PEI (N-C-C) with oxygen of water molecule.

RDF for number of water molecule surrounding the protonated PEI backbone is calculated to ascertain the number of water molecule surrounding linear PEI chain. Three distinct peaks are obtained at 0.28 nm, 0.35 nm and 0.46 nm. In case of system C, highest peak is obtained which implies that number of water molecule surrounding polymer backbone is highest in that case. While PEI in system C is surrounded by lowest number of water molecule. It is consistent with the previous observation that PEI is not present deep inside the hydrophilic head group of the bilayer as compared to PEI in system D. When PEI is slightly away from the hydrophilic part of the bilayer, it is interacting with more number of water molecules. While when the PEI is present deep into the hydrophilic head of the lipid group, it is surrounded by less number of water molecules. For system E, number of water molecule surrounding is just higher than in the system B. RDF for system E indicates that protonated PEI is surrounded by sufficient number of water molecule which is supported by the fact that water is present in the hydrophobic region of the bilayer. Now, it can be said that water present in the hydrophobic region of the bilayer is surrounding the PEI molecule.

3.6 Hydrogen bonds in unprotonated case:

As we observed that structure of unprotonated PEI was more coiled in system A than in system B. We calculate the number of intermolecular hydrogen bond which PEI makes with water of the lipid bilayer and also intra-molecular hydrogen bond of PEI. Hydrogen bonds are determined based on cut-offs for the angle Acceptor- Donor – Hydrogen and the distance Hydrogen – Acceptor. It was seen that when PEI was in more coiled conformation in system A, it makes intra-molecular hydrogen bond with itself, whereas no intra-molecular hydrogen bonds of PEI were observed in system when it has open conformation. Number of hydrogen bonds which PEI makes with water also decreases when PEI has coiled conformation.

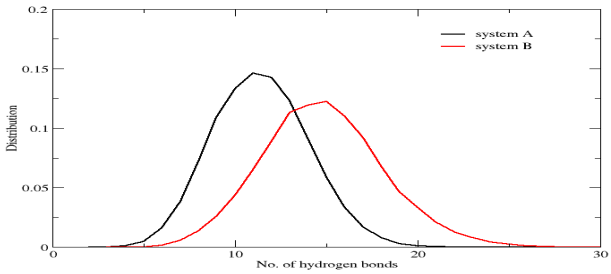

Figure15. Distribution of number of hydrogen bonds between PEI and water molecule in system A and B.

The numbers of hydrogen bonds were counted in each frame during last 50ns of the simulation.

The average number of hydrogen bond between PEI and water molecule was equal to 11 for system A and 15 for system B. It implies that when PEI was in more coiled conformation in system A, it has interaction with less number of water molecules and there is a competition between formation of intermolecular and intra-molecular hydrogen bond formation.

3.7 Centre of Mass coordinates of PEI: X, Y and Z-coordinates of COM of PEI are plotted for complete 150ns of simulation.

i) Unprotonated Case:

a) PEI in water (system A)

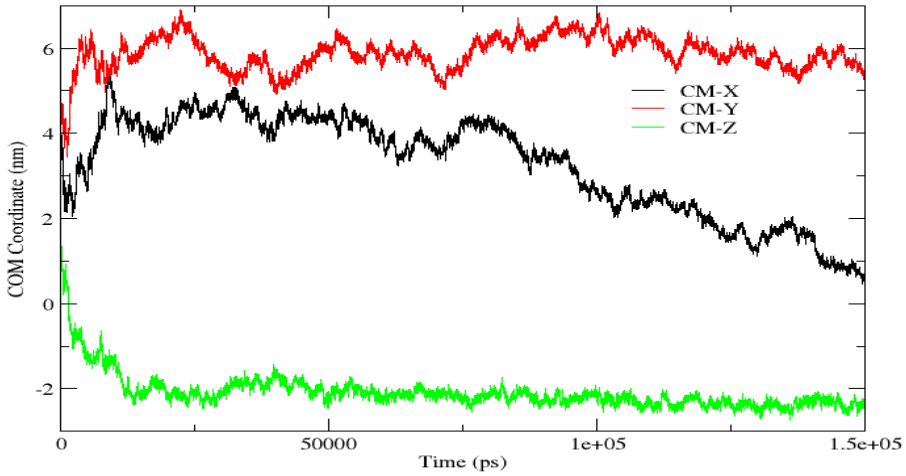

Figure 16. Plot of x, y and z-coordinate of centre of mass of PEI with respect to time in system A

It was observed that the centre of mass of PEI along the z-direction is almost constant after fluctuation during initial few ns of simulation. We started with the coiled conformation of unprotonated PEI placed slightly away from the head group part of PEI. Once it starts interacting with the lipid head group, its centre of mass coordinate is almost constant after that time. PEI stays near the head group region till the end of the simulation.

b) PEI in bilayer

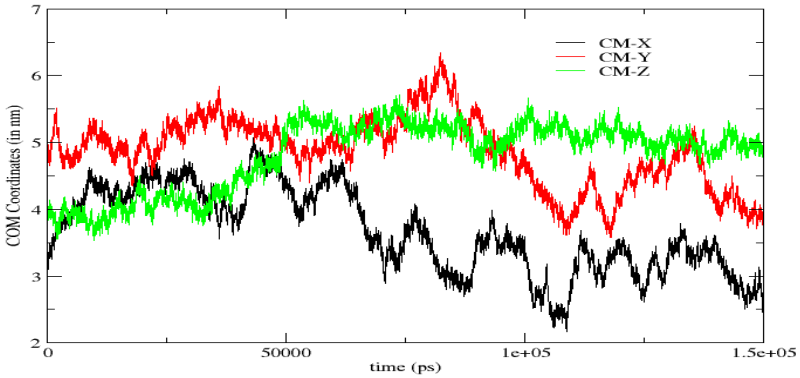

Figure 17. Plot x, y and z-coordinate of centre of mass of unprotonated

PEI in system B.

In case of system B, PEI was placed near the centre of the bilayer, as shown in figure 15, its centre of mass along the z-direction was nearly equal to 4nm. Position of PEI is in the middle of the bilayer for starting around 35ns. After this time, PEI interacts with some water molecule and then it was pulled towards lipid head group region and never came back to hydrophobic part of the bilayer again. The z-coordinate of centre of mass of PEI explains that the PEI was associated with the lipid head group region of the bilayer.

Centre of mass of Protonated PEI:

i) Protonated PEI in water (system C)

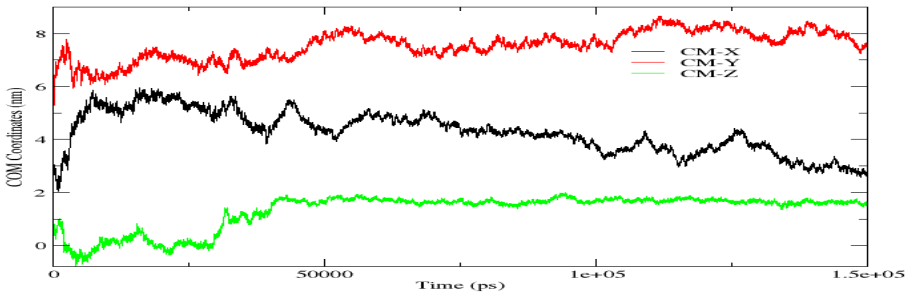

Figure 18. Plot of x, y and z-coordinate of centre of mass of protonated PEI in system C.

We started the simulation for system C by positioning linear PEI few angstroms away from the lipid head group region. After around 50ns of simulation, centre of mass co-ordinate of protonated PEI along the z-direction reached an equilibrium value. The association of linear PEI with the bilayer head group is favoured.

ii) Protonated PEI in bilayer (System D):

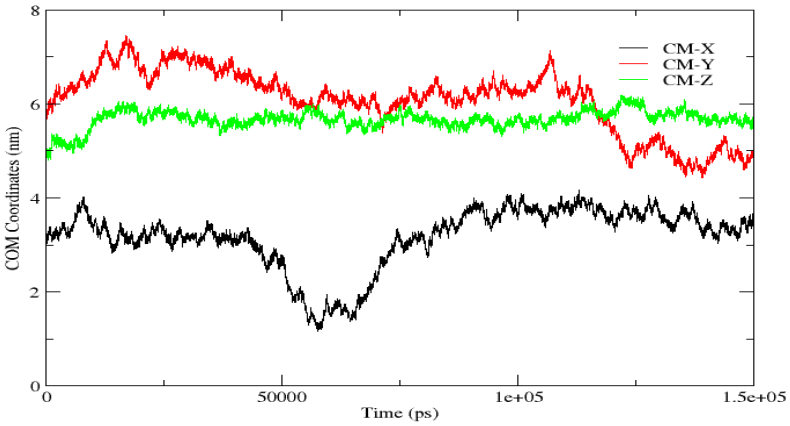

Figure 19. Plot of x, y and z-coordinate of centre of mass of protonated PEI in system D.

In the initial structure for system D, protonated PEI was placed in the middle part of the bilayer. But we can see from the plot that the z-coordinate of centre of mass of PEI starts to drift from the beginning of the simulation. It indicates that protonated PEI has large amount of favourable interaction with the water and the lipid head group and staying of protonated PEI in hydrophobic part of the bilayer is unfavourable.

iii) Protonated PEI placed along the normal of the bilayer:

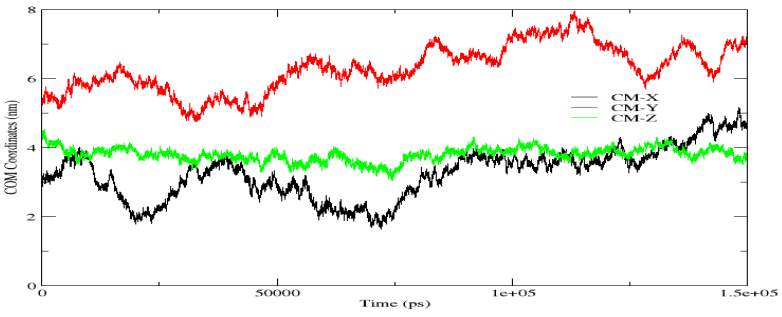

Figure 20. Plot of x, y and z-coordinate of centre of mass of protonated PEI in system E.

In system E, Position of centre of mass along the z-direction is almost in the middle of the bilayer. It indicates that PEI position is almost same till the end of the simulation and the forces were balanced to keep it in the same position.

Pore formation along the bilayer:

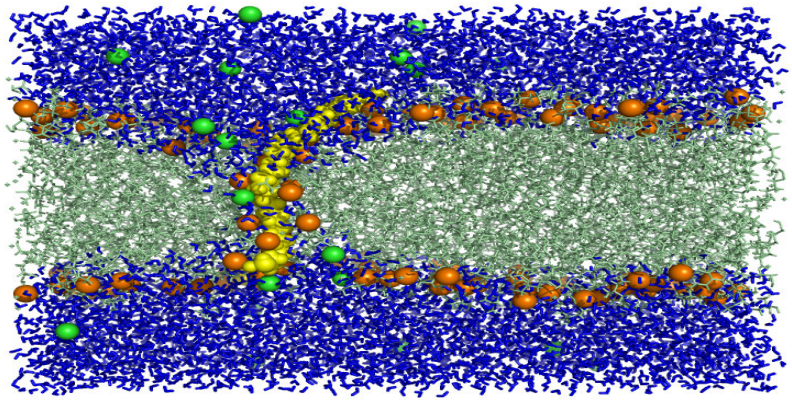

Figure 21. Pore formation in system E.
Snapshots taken in yz plane. Water as blue sticks, PEI as yellow spheres, lipid tail in pale green colour, P atoms as orange colour spheres, and chloride ions as green sphere.

Here we will discuss about system E, where pore formation in the bilayer was observed. From the snapshots of system E, It was seen that water molecules passing through the bilayer and it is surrounding the protonated PEI molecule. It was observed that many lipid groups were present in the hydrophobic region of the bilayer and water was flowing through the bilayer. To characterize the environment of linear PEI, we plotted radial distribution function for backbone of PEI (N-C-C) with the phosphorus of the lipid molecule and oxygen of water molecules. The plot is shown below, indicating a similar environment for PEI in system D and E. The number of lipid molecule present in the inner region of the bilayer is 6 to 7, which is same number as reported by Kepczynski et al.[26] where 14 lipid molecule were present in the region between the bilayer in presence of two polycation molecules. The inner region was defined as region 0.2 nm above from the middle of the bilayer. A DOPC molecule was counted as present in the inner region of the bilayer if its P

atom of lipid head group is present in the defined region. The water molecule starts penetrating the bilayer from the starting few picoseconds of the simulation and significant number of water molecules are present in the inner region of the bilayer from the beginning of the simulation.

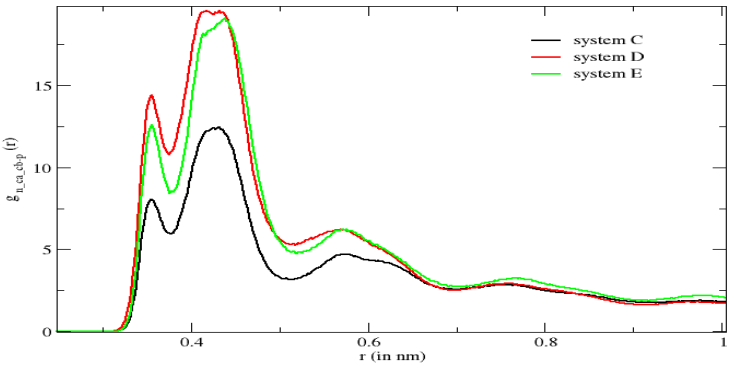

Figure 22. Radial distribution function plot for backbone of PEI with the P atom of the lipid molecule.

The radial distribution function for phosphorus atom around the backbone of the polymer shows three distinct peaks at around 0.36 nm, 0.43 nm and 0.57 nm. The first and third peak corresponds to N-P distance whereas 2nd peak corresponds to C-P distance. The height of the peak was almost same for system D and E. It implies that number of phosphorus atoms surrounding the chain were same for protonated PEI in system D and E. It proves that protonated PEI is able to deform the bilayer when it is inserted into it. As the head group move towards inside of the bilayer leading to deformation of part of the bilayer due to presence of protonated PEI chain. It can be said that when protonated PEI will be present in large concentration, there will be large deformation in the bilayer structure.

Snapshots of each system at different time during the simulation:

Snapshots of different system at different times:

1) Snapshots of system A at a)0ps, b) 10ns, c) 40ns, d) 150ns)

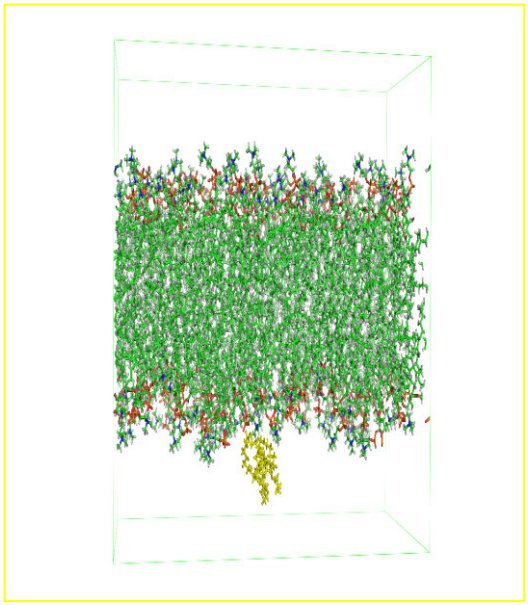

At 0ns. Water has been removed for clarity. PEI chain is in yellow colour.

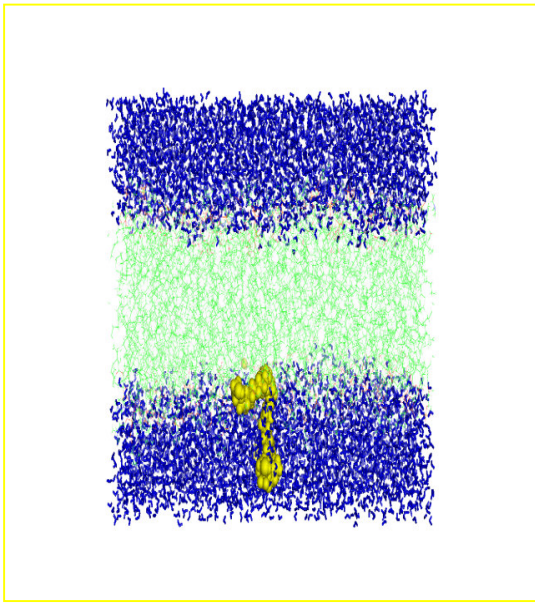

At 10 ns. Water has been shown in blue colour.

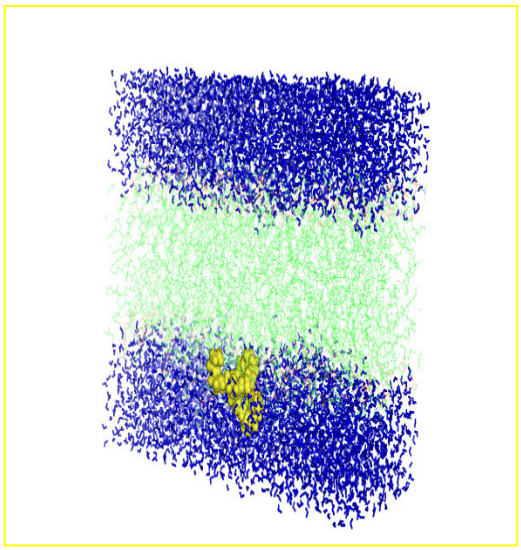

At 40ns, part of PEI is interacting with the lipid head group

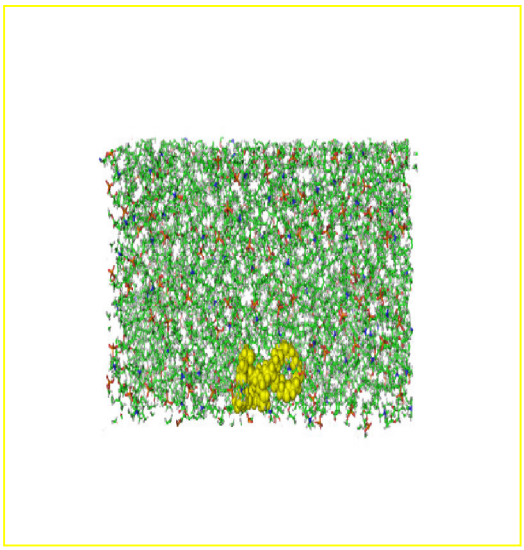

At 150ns. Top view along the z-direction showing coiled structure. Water has been removed for clarity.

Figure23. Snapshots of system A

2) System B (Unprotonated PEI in bilayer) at 0ns,35ns,60ns,150ns

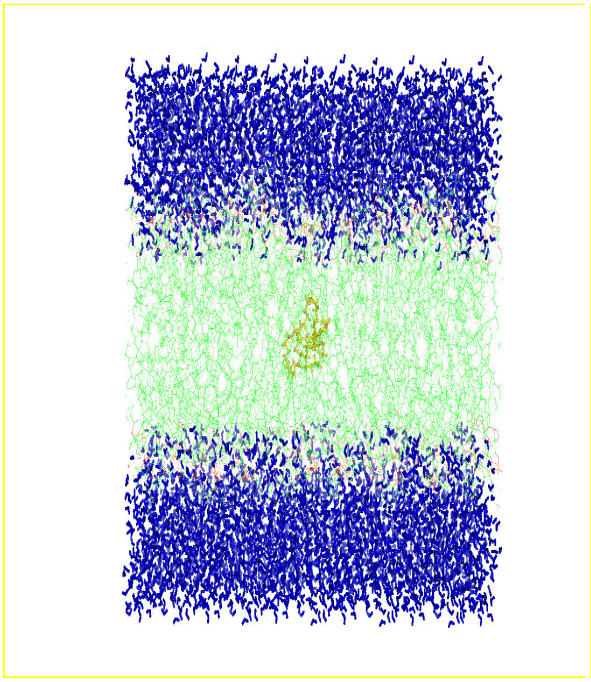

At 0ns. PEI is placed in the middle of the bilayer.

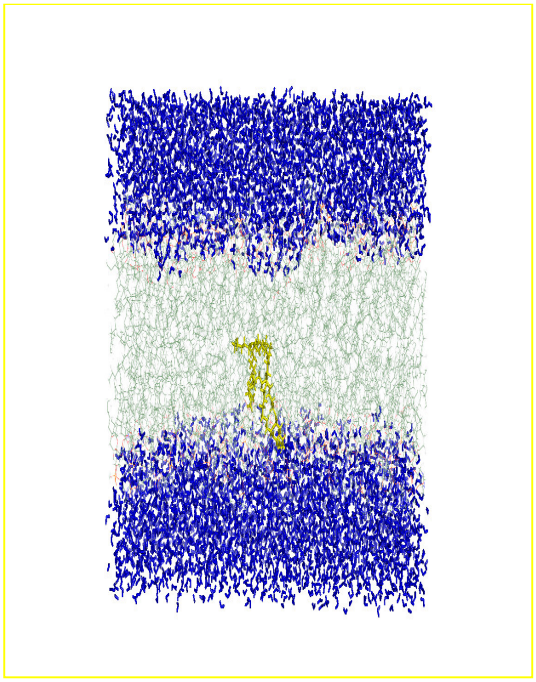

At 35ns, a part of PEI is interacting with the lipid head group.

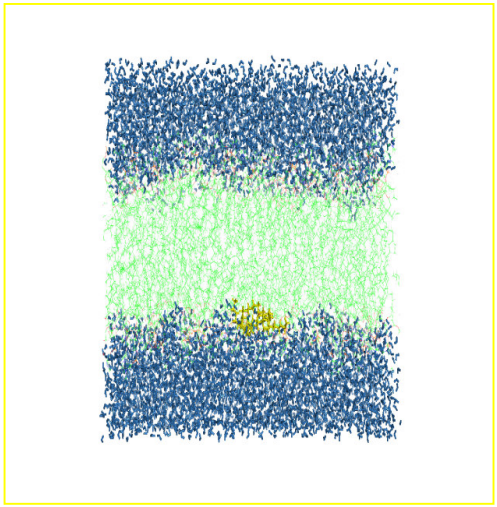

At 60ns, complete PEI is present in the hydrophilic region of the bilayer.

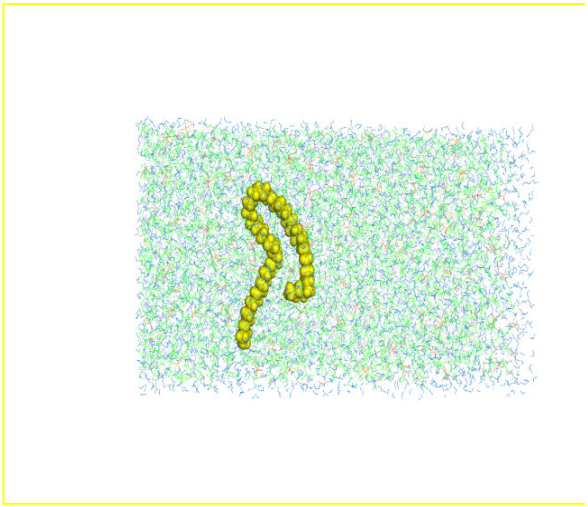

At 150ns, PEI showing no coiling in its structure.

Figure 24. Snapshots of system B

3) System C (Protonated PEI in water)

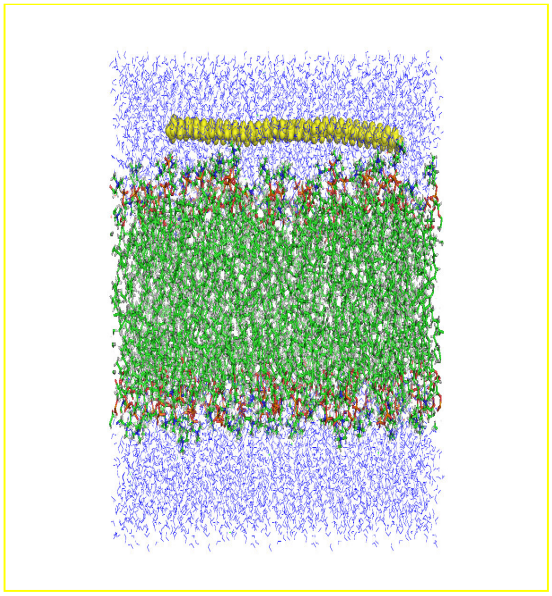

At 0ns. PEI is placed slightly away from the head group.

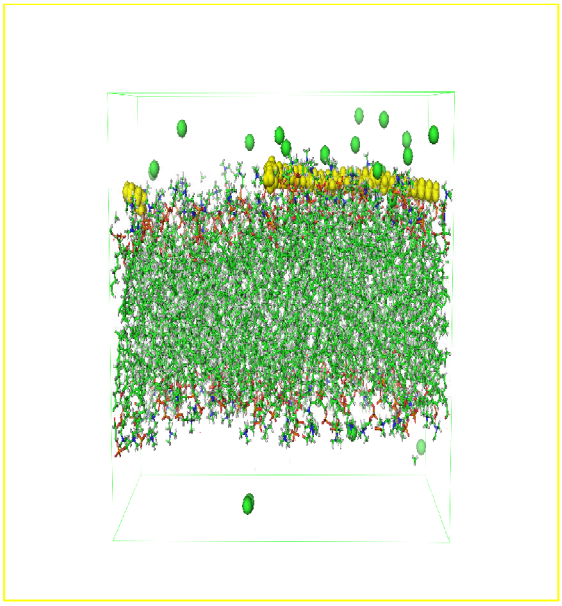

At 150ns. PEI is attached to lipid head group.

Figure25. Snapshots of system C

4) System D (protonated PEI in bilayer) 0.5 ns (position restraint),10ps, 5ns, 100 ns

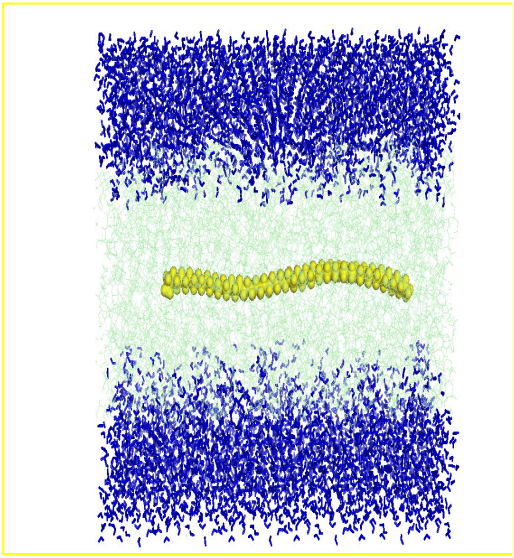

At 0ns, PEI is present in the middle part of the bilayer

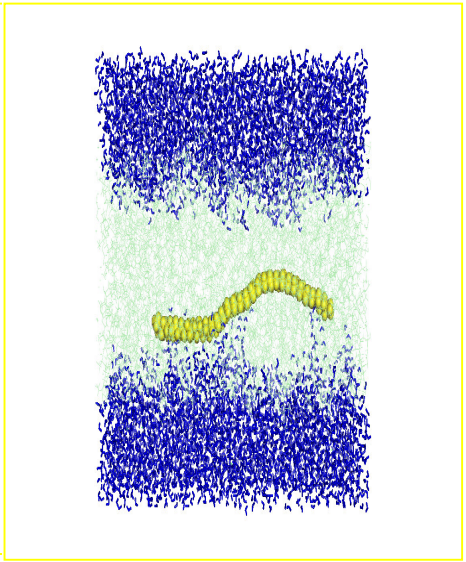

At 10ps, PEI starts to drift towards head group of lipid.

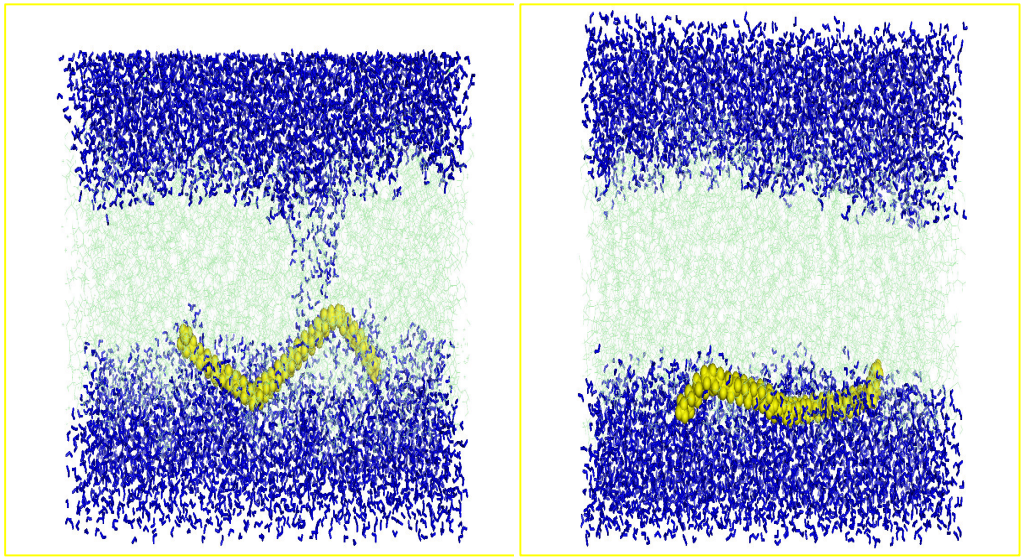

At 5ns, water is moving across the bilayer to solvate the PEI molecule.

At 150ns, protonated PEI is completely shifted towards one leaflet of the bilayer.

Figure26. Snapshots of system D

5. Snapshot for System E at (0 ps, 100ps, 50ns, 150ns)

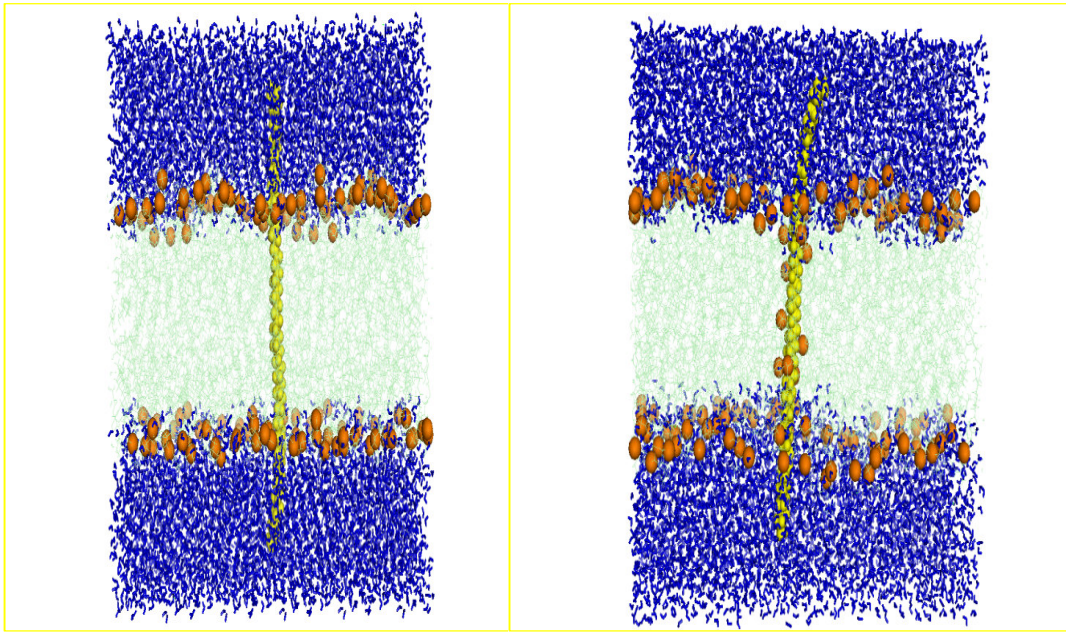

At t = 0ps

At t = 100ps

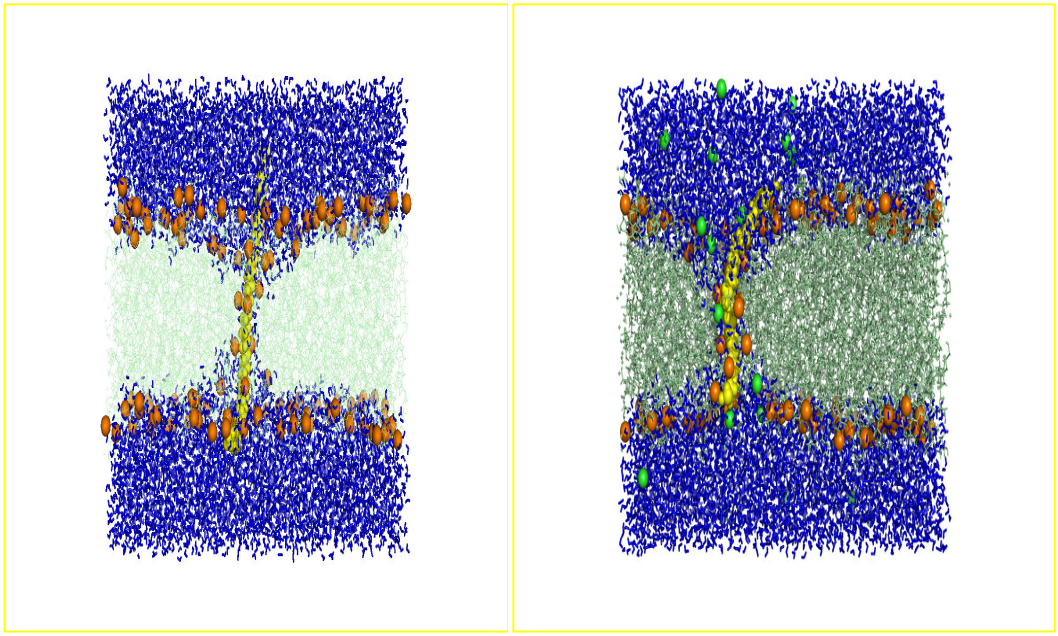

At t = 50ns At t = 150ns

Figure27. Snapshots of system E

Discussion:

To explore the effect of interaction of PEI with lipid bilayer at different pH condition, we designed five different systems. Different pH condition had been incorporated by taking two different structure of PEI. It is known that at different pH, structure of PEI is different. It was expected that they will interact differently with the membrane. We aimed to find out which part of lipid bilayer has favourable interaction with PEI. As unprotonated PEI has N atom and also there are double the number of carbon atom, it has both hydrophobic and hydrophilic part present in it. As lipid bilayer also has both hydrophobic and hydrophilic part, it would be interesting to see the final position of PEI in the lipid bilayer region, starting with different initial position of PEI. So, we started with two different position of coiled PEI in system A and B. In system A, unprotonated PEI was present in water above the lipid head group and in system B, unprotonated PEI was present deep in to the hydrophobic part of the bilayer. In the first few nanosecond of simulation for system A, coiled PEI stays in water above the lipid head group. But, after around 10ns, unprotonated PEI starts to interact with the lipid head group as shown in figure 23. And soon complete PEI molecule interacts

with the head group of the bilayer. And then it never goes away from the lipid head group region. Also, in case system B coiled PEI has constrained motion in the hydrophobic core region of the bilayer at the beginning of the simulation, but after around 40ns, part of the molecule sees some water, and after that complete PEI molecule was pulled towards the lipid head group. But once it reaches the hydrophilic lipid head region of the bilayer, it stays there till the end of the simulation. It is clear that once unprotonated PEI is near the lipid head group, it attaches to that part of the bilayer. And there is no further movement along the normal of the bilayer. At the end of simulation, PEI in both systems has reached at the same positions as indicated by the density plot of the systems, but there are differences in structure of PEI in equilibrated configuration of system A and B. The PEI in system A had closed structure, supported by lower R_g and E2E distance. The E2E and R_g distribution suggest that there are two conformations for PEI in system A, both of which have significantly more coiled conformation. The preference for extra coiled conformation can be investigated in further study. PEI in system A had more coiled conformation and hence surrounded by less number of water molecules, whereas PEI in system B has open conformation and hence surrounded by more number of water molecule. Unprotonated PEI in system B forms more number of hydrogen bond with water than PEI in system A. The coiled structure also shows the presence of intra-molecular hydrogen bonds while there are no such intra-molecular hydrogen bonds in PEI of system B, due to open structure during last 50ns of the simulation. It has been reported that polymer interact with bilayer via hydrophobic interaction, hydrogen bond and coulombic association. Here, in system A and B, The interaction of PEI with head group is mainly driven by electrostatic interaction.

When we performed the simulation for protonated PEI with bilayer in system C, D and E, there was no change in area per lipid for system C and D but there was a significant increase in area per lipid for system E. It implies that a single chain of PEI can significantly increase the area per lipid if it inserts into the membrane, whereas attachment of single chain with head group didn't significantly change the area per lipid of the bilayer. The conformation of PEI was linear when it was attached to head group of the bilayer as in the starting structure in system C and D. whereas it is bent towards lipid head group in the case of system E. The linear PEI is not able to go deep into bilayer head group when it is placed as shown in the figure for system C. It

can be said that there is favourable interaction between lipid head group and PEI but it seems that it is difficult for a large molecule to enter the membrane without proper orientation. The R_g and E2E distribution plot of the polymer in system D and E are same, also rdf plots showing water and head group positions around which indicates that PEI in both the system have similar structure, whereas PEI in system C is more elongated when it is slightly away from the hydrophilic head group. The pore formation in case of system E was observed. The lipid molecules were oriented towards the protonated PEI molecule from the starting few picoseconds of simulation. The considerable increase in area per lipid was observed in case system E due to entry of water molecule inside the bilayer.

Conclusion:

Unprotonated PEI attaches to the hydrophilic head group region of the bilayer. Although initial positions of PEI were biased towards hydrophobic and hydrophilic part of the bilayer in two different systems A and B, the unprotonated PEI showed a preference towards interaction with the hydrophilic head of the bilayer. The unprotonated PEI doesn't cause to change the area per lipid of the bilayer significantly and bilayer structure remain intact on interaction of single chain of unprotonated PEI with the bilayer. Unprotonated PEI in system A and B has different conformation at the end of the simulation although they are at the same position along the z-axis of the bilayer. Unprotonated PEI in system A is more coiled and facing less number of water molecules whereas PEI in system B has relatively open structure and is surrounded by more number of water molecule. It is predicted that both conformations of unprotonated PEI are stable in the hydrophilic head group region of the bilayer.

Protonated PEI also attaches to the hydrophilic head group region of the bilayer. The protonated PEI is not able to insert into the membrane for the system C, where it was placed perpendicular to normal as shown in figure 25. It indicates a proper orientation is necessary to enter PEI into the bilayer. The protonated PEI when attached with the head group region of the bilayer towards one leaflet of the bilayer didn't result in increase in area per lipid for the bilayer system. But in case of

protonated PEI placed along the normal of the bilayer in system E, pore formation was observed and this caused an increase in lateral area of simulation box and hence an increase in area per lipid. It is concluded that PEI is able to form a stable pore in the bilayer. The density profile for protonated PEI with bilayer is almost same for all the system except the case when the pore formation was observed. There is a channel formed surrounding the protonated PEI molecule, water molecules and chloride ions flows through that channel. There is reorientation of lipid molecule surrounding the PEI chain such that lipid molecules are tilted towards PEI to help forming a pore. Six DOPC molecules are involved in forming the pore which are present in the apolar region of the bilayer. Protonated PEI has expanded structure when it is slightly away from the hydrophilic head group in system C compared to case of system D and E, where PEI molecule is completely surrounded by hydrophilic head group of the bilayer. It is finally concluded that a single protonated PEI causes significant change in bilayer orientation when inserted inside the bilayer. When protonated PEI is present in high concentration then a large change in bilayer structure is expected.

References:

1. Alberts B, Johnson A, Lewis J, et al. Molecular Biology of the Cell. 4th edition. New York: Garland Science; 2002.
2. Boussif, O.; Lezoulac'h, F.; Zanta M. A.; Mergny, M. D.; Scherman, D.; Demeneix, B.; Behr J. P. Proc. Nat. Acad. Sci. USA. 1995, 92, 7297-7301.
3. Brissault B, Kichler A, Guis C, et al. Bioconjug Chem 2003; 14: 581–587.
4. Jones GD, Langsjoen A, Neumann MMC, et al. J. Org. Chem. 1944; 9:125–147.
5. Suh J, Paik HJ, Hwang BK. Ionization of poly(ethylenimine) and poly(allylamine) at various pHs. Bioorg. Chem. 1994; 22:318–327.
6. Behr, J. P.; Chimia 1997, 51, 34-36.
7. Sharma K. P.; Choudhary C. K.; Srivastava S.; Davis H.; Rajamohan P. R.; Roy S., Kumaraswamy G. J. Phys. Chem. B, 115, 9059-9069
8. Biophysical Journal Volume 73 November 1997 2269-2279.
9. Small, D. M. 1986. The Physical Chemistry of Lipids: From Alkanes to Phospholipids. Plenum Press, New York.
10. Holte et al. Biophysical J.68, 1995, 2396-2403.
11. Cavazzana-Calvo,M.; Hacein-Bey, S.; De.Saint Basile G.; Gross, F.; Yvon, E.; Nusbaum, P.; Selz,F.; Hue, C.;Certain, S.; Casanova, J. L.; Bousso,P.;Le Deist, F.; Fisher, A. Science 2000, 288, 669-672.
12. Yang, Z.R.; Wang, H.F.; Zhao, J.; Peng Y. Y.;Wang, J.; Guinn, B.-A.; Huang, L.Q. Cancer Gene Ther 2007, 14, 599-615.
13. Parhamifar, L.; Larsen, A. K.; Hunter, C.; Andersen, T. L.; Moghimi, S. M. Soft Matter, 2010, 6, 4001-4009.
14. Mulligan, R. C.; Science 1993, 260, 926-932.
15. Check E.; Nature 2002, 420, 116-118.
16. Meintzer M. A.; Simanek E. E. Chem. Rev. 2009,109, 259-302.
17. Bloomfield A. V. Curr Opin Struct Biol 1996, 6, 334-341.
18. Khalil I. A.; Kogure K.; Akita H.; Harashima H.; Pharamacol. Rev. 2006, 58, 32-45.
19. Behr, J. P.; Chimia 1997, 51, 34-36.
20. Sonawane N. D.; Szoka F. C. Jr; Verkman A. S. J Biol Chem 2003, 44826-44831.

21. Kichler A.; Leborgne C.; Coeytaux E.; Danos O.; J Gene Med 2001, 3, 135-144.
22. Itaka, K.; Harada A.; Yamasaki, Y.; Nakamura, K; Kawaquchi, H; Kataoka, K. J Gene Med 2004, 6, 76-84.
23. Tribet C.; Vial F. Soft Matter 2008, 4, 68-8.
24. Sikor M.; Sabin J.; Keyvanloo A.; Schneider M. F.; Thewalt J. L.; Bailey A. E.; Frisken B. J. Langmuir 2010,26(6),4905-4912.
25. Lee H.; Larson R. G. J. Phys. Chem. B 2006,110, 18204-18211.
26. Kepczynski M.; Jamroz D.; Wytrwal M.; Bednar J.; Rzad E.; Nowakoska M. Langmuir 2012,28(1),676-688.
27. Siu S. W. I.; Vacha R.; Jungwirth P.; Bockmann R. A.; J. Chem. Phys. 2008,128, 125103.
28. S.J. Weiner, P.A. Kollman, D.A. Case, U.C. Singh, C. Ghio, G. Alagona, S. Profeta, P. Weiner J. Am. Chem. Soc. 106 1984 765–784.),
29. B.R. Brooks, R.E. Bruccoleri, B.D. Olafson, D.J. States, S. Swaminathan, M. Karplus, J. Comp. Chem. 42, 1983, 187–217.
30. van Gunsteren W.F., Kruger P., Billeter S.R., A.E., Eising A.A., W.R.P., Scott P.H. Huneberger, Tironi I.G., Biomolecular Simulation: The GROMOS96 Manual and User Guide, BiomosrHochschulverlag AG an der ETHZurich, GroningenrZurich, 1996.
31. Jorgensen W.L., Tirado-Rives J., J. Am. Chem. Soc. 110,1988,1657–1666.
32. D. van der Spoel, E. Lindahl, B. Hess, A. R. van Buuren, E. Apol, P. J. Meulenhoff, D. P. Tieleman, A. L. T. M. Sijbers, K. A. Feenstra, R. van Drunen and H.J.C. Berendsen, Gromacs User Manual version 4.5.4, www.gromacs.org (2010)
33. Allen M.P.; Tildesely D.J. Computer Simulation of Liquids, Clarendon Press, Oxford, 1987.
34. Hess, B., Bekker, H., Berendsen, H. J. C., Fraaije, J. G. E. M. LINCS: A linear constraint solver for molecular simulations. J. Comp. Chem. 18:1463–1472, 1997
35. Ryckaert, J-P; Ciccotti G, Berendsen HJC (1977). *Journal of Computational Physics* 23 (3): 327–341)
36. Leach Andrew R. Molecular Modelling: principles and applications. 2nd edition, Pearson Education, 2001.

37. a)Byrd, R. H., Lu, P., Nocedal, J. A limited memory algorithm for bound constrained optimization. SIAM J. Scientif. Statistic. Comput. 16:1190–1208, 1995. b) van Gunsteren, W. F., Berendsen, H. J. C. A leap-frog algorithm for stochastic dynamics.Mol. Sim. 1:173–185, 1988.
38. Berendsen, H. J. C., Postma, J. P. M., DiNola, A., Haak, J. R. J. Chem. Phys. 81:3684–3690, 1984.
39. Bussi, G., Donadio, D., Parrinello, M. J.Chem. Phys. 126:014101, 2007.
40. Nos´e, S. Mol.Phys. 52:255–268, 1984.
41. Hoover, W. G. Phys. Rev. A 31:1695–1697, 1985.
42. (a) van der Spoel, D.; Lindahl, E.; Hess, B.; Broenhof, G. J. Comput. Chem. 2005, 26, 1701–1718. (b) Lindahl, E.; Van der Spool, D.; Kutzer, C.; Hess, B. J. Chem. Theory Comput. 2008, 4, 435–447. (c) http://www.gromacs.org
43. Berendsen, H. J. C.; Postma, J. P. M.; van Gunsteren, W. F.; DiNola, A.; Haak, J. R. J. Chem. Phys. 1984, 81, 3684-3690.
44. Hess, B.; Bekker, H.; Brendensen, H. J. C.; Fraaije, J. G. E.M. J. Comput. Chem. 1997, 18, 1463-1472.
45. Miyamoto S.; Kollman P. A. J Comput. Chem. 1992,13, 952